Chinese Journal of Electronics
Vol.32, No.2, Mar. 2023

On-Chip Reconfigurable Microwave Photonic Processor

ZHANG Weifeng[1,2,3,4] and WANG Bin[1,2,3,4]

(1. *Radar Research Lab, School of Information and Electronics, Beijing Institute of Technology, Beijing 100081, China*)
(2. *Key Laboratory of Electronic and Information Technology in Satellite Navigation (Beijing Institute of Technology), Ministry of Education, Beijing 100081, China*)
(3. *Beijing Institute of Technology Chongqing Innovation Center, Chongqing 401120, China*)
(4. *Chongqing Key Laboratory of Novel Civilian Radar, Chongqing 401120, China*)

Abstract — Microwave photonic processors leverage the modern photonics technique to process the microwave signal in the optical domain, featuring high speed and broad bandwidth. Based on discrete optical and microwave components, different microwave photonic processors are reported. Due to the limitation of the optoelectronic components, most of the realized processors are designed to serve a specific demand. With the booming development of photonic integrated circuits (PICs), new possibilities are opened for the implementation of integrated microwave photonic processors. By using the high-precision planar fabrication process, on-chip microwave photonic processors are enabled to have unprecedently full reconfigurability to perform multiple processing tasks. An overview regarding our recent work on reconfigurable microwave photonic processors is presented with an emphasis on silicon photonics integrated solutions.

Key words — Integrated microwave photonics, Reconfigurable signal processor, Bragg grating, Micro-disk resonator.

I. Introduction

Microwave photonic signal processing is a topic of interest in microwave photonics field [1]–[4]. With the use of modern photonics, microwave signal is processed in the optical domain, which opens up new possibilities for overcoming the speed and bandwidth limitations in conventional electrical signal processors [5]–[8]. In the past two decades, extensive studies have been conducted and various demonstrations have been reported. Different signal processors including microwave photonic filters [9], [10], photonic fractional-order temporal differentiators and integrators [11], [12], Hilbert transformers [13], microwave photonic mixers [14], [15], microwave phase shifters [16], [17], pulse shapers [18]–[20], and true time-delay beamforming network [21] have been successfully demonstrated.

However, most of the demonstrated signal processors are implemented with the use of discrete optical and microwave components, which leads to a poor stability and large power cost. Meanwhile, these processors were designed for a specific signal processing task. To reduce the cost of application-specific processors, a reconfigurable signal processor that can be field-programmed on demand for different tasks, like a widely-used field-programmable electronic FPGA signal processor, is highly preferred. With the rapid maturity and growth of development in the photonic integrated circuits (PICs), a promising approach is enabled to realize chip-scale integration of microwave photonic signal processors, which is becoming a hot research topic [22]–[25]. Thanks to its high-density and high-precision integration offered by PIC technology, multiple different optoelectronic components can be integrated on a single circuit chip, which makes a reconfigurable microwave photonic processor possible with a compact footprint, high stability, and high-precision manipulation capability.

The first on-chip programmable photonic signal processor was proposed by Zhuang and his colleague on a silicon nitride chip, which has a two-dimensional mesh network consisting of a grid of tunable Mach–Zehnder interference (MZI) couplers [26]. By controlling the MZI couplers, different circuit topologies are resulted and

Manuscript Received Aug. 31, 2020; Accepted July 18, 2022.
 DOI:10.23919/cje.2020.00.273

hence multiple signal processing functions are performed with the signal processor. Subsequently, different mesh structures, such as hexagonal and triangular-shaped meshes, were also proposed on a silicon photonic chip to realize the programmable photonic signal processor [27]. However, since an MZI coupler usually has a large size, to reduce the footprint of the processor, a reconfigurable photonic integrated signal processor was proposed with the use of three compact micro-ring resonators (MRRs) on an InP chip. With the currents injected into the active components, the signal processor can be reconfigured to performing different signal processing functions. In the report [28], three functions including temporal integration, temporal differentiation and Hilbert transformation are experimentally demonstrated.

By leveraging the mature and monolithic CMOS process, silicon photonics is envisioned as a promising opto-electronic integrated platform. In this paper, we will discuss three silicon-based reconfigurable microwave photonic signal processor. Specifically, a programmable waveguide grating based on distributed PN junctions will be presented, and the use of the grating in a microwave photonic system for reconfigurable microwave signal will be discussed. To realize the multiple channel signal processing, an on-chip programmable multi-channel grating based on equivalent phase-shifted grating technique is designed, fabricated and demonstrated. In addition, to make a smaller size of the microwave photonic processor chip, a programmable micro-disk resonator (MDR) array photonic signal processor is also presented. Finally, a discussion is given and the conclusion is drawn.

II. Programmable Waveguide Bragg Grating

Bragg gratings are created by introducing the periodic variations of the refractive index along the optical propagation, which enable selective reflection of the lightwave signals. In principle, the spectral response of a grating depends on its index modulation profile. By designing the profile, the spectral response of the gratings can be specified. Since the invention of the Bragg gratings, owing to its easy fabrication and strong filtering capability, Bragg gratings are widely used as versatile optical filters in various scientific and industrial fields.

Fig.1 shows the schematic of a silicon-based programmable waveguide grating, which is divided into multiple uniform Bragg gratings and a straight waveguide as a resonant cavity region [29]. The grating structure are realized by etching periodic teeth on the waveguide sidewall. To realize the tuning of the waveguide refractive index locally, multiple distributed lateral PN junctions are incorporated, and each junction owns an independent electrode. When a bias voltage is applied to a specific PN junction, the refractive index of the silicon waveguide can be adjusted locally. Therefore, by controlling all the applied voltages, the grating index modulation profile could be reconfigured, which makes the grating have a programmable spectral response for various applications.

Fig.2 shows the fabricated chip image which is captured using a microscope camera. The grating is designed to have three regions: one uniform sub-gratings, a straight waveguide as a resonant cavity region and another identical uniform grating. Each region incorporates an independent lateral PN junction to tune the local waveguide refractive index. Fig.2(a) shows the image of the fabricated entire programmable waveguide grating. The optical I/O is realized with three grating couplers, and a 3-dB Y-branch is used to collect the reflected light. Fig.2(b)–(f) presents a zoomed-in view of the grating coupler for the input optical signal coupling, the 3-dB Y-branch for collecting the optical signal reflection, the transmission and reflection grating couplers for coupling the optical signal out of the chip, the left uniform sub-gratings with 2000 grating periods, the resonant cavity waveguide as long as 14.6 μm, and the right uniform sub-gratings with 2000 grating periods, respectively. By collaboratively controlling the bias voltages on the PN junctions, the entire grating index modulation profile can be reconfigured on demand, and thus its spectral response can be tailored for different applications.

With the fabricated programmable waveguide grat-

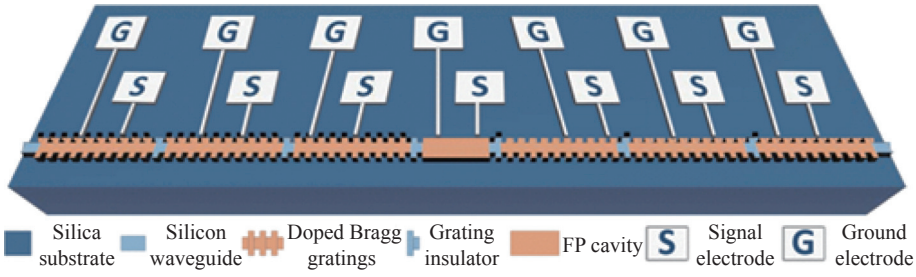

Fig. 1. Schematic of a programmable waveguide grating.

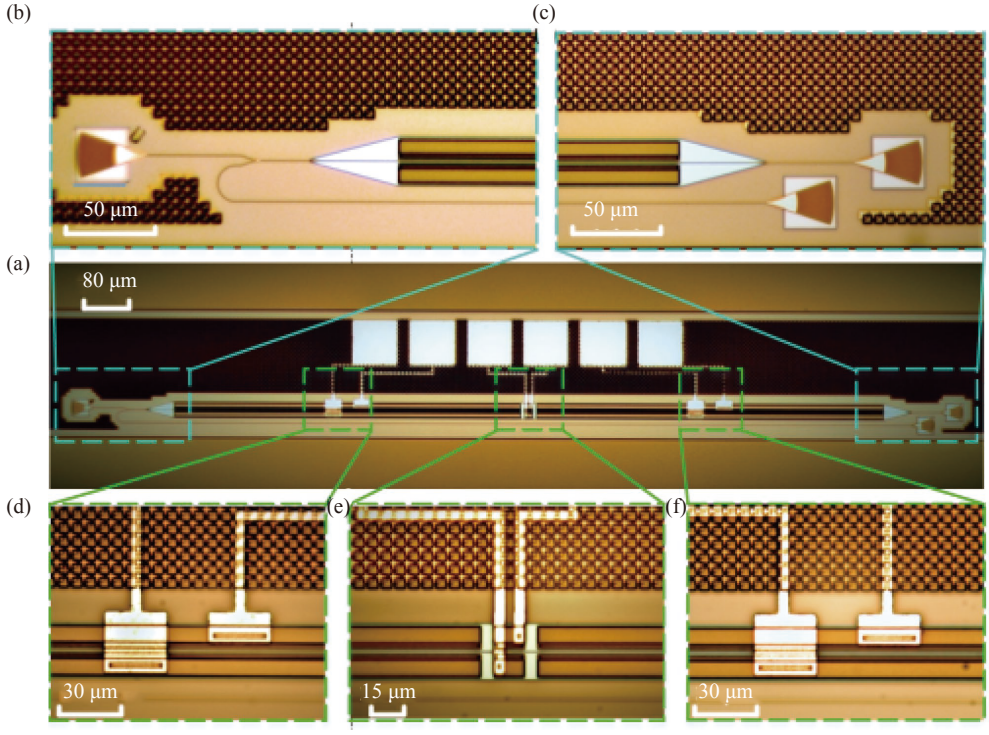

Fig. 2. Images of the fabricated silicon-based programmable waveguide grating using a microscope camera. (a) Whole grating; (b) Input region; (c) Transmission and reflection output regions; (d) Left uniform sub-gratings; (e) Straight waveguide as a resonant cavity region; (f) Right uniform sub-gratings.

ing, different grating spectral response can be realized. First, in the static state, the existence of the FP cavity in the middle can introduce a phase shift, which helps the fabricated grating to be a phase-shifted grating. Fig.3(a) shows the measured reflection and transmission spectra, in which a resonant window occurs within the stopband in the transmission spectral (in red), and a notch is located in the passband in the reflection spectral (in blue). This is a unique feature of a phase-shifted Bragg grating. When the PN junctions in the two sub-gratings are synchronously tuned, the notch wavelength is shifted as shown in Fig.3 (b). According to the free-carrier plasma dispersion effect on silicon, the concentration change of the free-carriers in the silicon waveguide gives rise to the change of the silicon waveguide refractive index, which eventually results in a shift of the Bragg wavelength. When a reverse bias voltage is used, the Bragg wavelength is red-shifted; when a forward bias voltage is used, the Bragg wavelength is blue-shifted. In addition to the notch wavelength shifting, the extinction ratio of the notch can also be tuned by controlling the three bias voltages. The blue-shift of the notch wavelength shift induced by reverse biased PN junction can be cancel out with the red-shift by the forward biased PN junction, while the different biased conditions of the three PN junctions induce a different roundtrip loss of the entire grating, which can be leveraged to tune the notch extinction ratio. Fig.3(c) presents the measurement results of the extinction ratio tuning. This is a distinct feature to be employed in the microwave signal processing.

Thanks to the increased optical absorption loss caused by the free-carrier injection into the PN junction, the fabricated waveguide grating is operated as a single uniform grating by disabling the optical-confining capability of the resonant cavity. Fig.3(d) shows the measured single uniform grating spectra when the right PN junction is forward biased with a large voltage. Lots of free-carriers are injected into the silicon waveguide, which leads to a heavy optical absorption loss in the waveguide transmission. As a result, the reflectivity of the right uniform sub-grating is heavily weakened, and only the left uniform sub-gratings work. Moreover, by applying a bias voltage of the PN junction in the left uniform sub-gratings, the Bragg wavelength of the uniform sub-gratings could be shifted as shown in Fig.3(e).

In addition to the free-carrier injection into the right PN junction, the free-carriers can also be injected into the PN junction of the FP cavity, which can also produce a uniform grating. Fig.3 (f) shows the measured uniform grating spectra when the PN junction of the FP cavity is forward biased with a large voltage. The optical spectral presents some uncommon features which are difficult or impossible to realize with the use of a traditional grating. This is definitely a distinct feature of the reconfigurable waveguide grating.

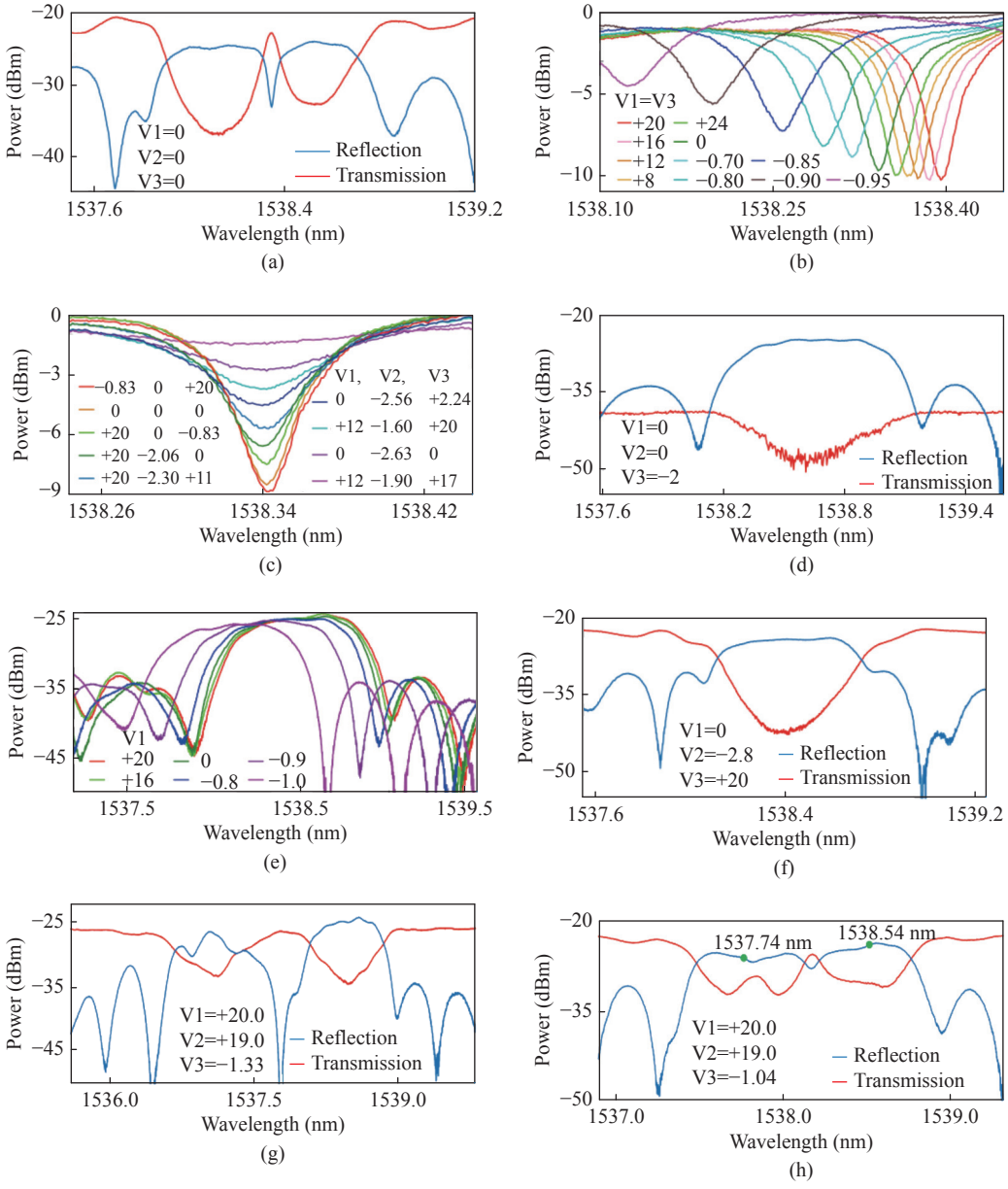

Fig. 3. (a) Static spectra of the fabricated waveguide grating; (b) Notch wavelength shifting of the notch; (c) Tunable notch extinction ratio; (d) Single uniform grating spectra; (e) Single uniform grating spectral shifting; (f) Another single uniform grating spectrum; (g) Two uniform gratings spectra; (h) Chirped grating spectrum.

Thanks to the independent tuning of the two uniform sub-gratings, it is straightforward to implement two uniform gratings when two PN junctions are biased at different conditions. For example, when the left PN junction is reverse biased, the left grating spectrum is red-shifted; meanwhile, the right PN junction is forward biased, which makes the right grating spectrum blue-shifted. Thus, two nonidentical uniform sub-gratings are implemented. Fig.3 (g) shows the measured spectra of two independent uniform gratings, in which two separate main reflection peaks can be seen apparently in the reflection spectrum. Furthermore, by cascading the reflection spectra caused by each uniform sub-grating, a chirped grating is produced. Fig.3(h) gives the measured spectral response of the realized chirped grating. Compared to the 3-dB bandwidth of the single uniform grating, the resulted chirped grating has a much broader spectral. Supposing the reconfigurable grating has an increased grating periods and incorporate more uniform sub-gratings, the resulted chirp grating would have a tunable chirp rate and group delay.

When the fabricated programmable grating is employed in a typical microwave photonic processor system, a reconfigurable microwave photonic processor is enabled, which can perform multiple signal processing tasks. For example, by reconfiguring the grating spectra, the signal processor can perform different single

processing tasks including fractional-order temporal differentiation, optical true time delay, and microwave photonic frequency identification [29]. In addition, with the use of the proposed grating, other tasks including microwave filtering, temporal integration, and Hilbert transformation can also be realized. Furthermore, by having more independent uniform sub-gratings, the signal processor can fulfill more tasks and the performance can also be improved.

III. Programmable Multi-Channel Waveguide Bragg Grating

With the explosive growth of data exchange, wavelength-division multiplexing (WDM), as a key technology, has been extensively leveraged in the current optical communications networks to expand the communication capacity. In a WDM optical network, multiple channel signal processing is usually required for ultrafast signal processing and characterization. However, in the above-mentioned programmable grating, the channel number is always one. With the use of nonuniformly spatial sampling on a uniform waveguide grating, an equivalent-phase-shifted (EPS) grating is resulted, which offers a potential solution to have a multi-channel processing capability. When the nonuniform spatial sampling profile is tuned, different spectral response of a high-precision EPS Bragg grating can be realized [30].

Fig.4(a) gives the schematic of a silicon-based reconfigurable EPS waveguide Bragg grating chip. By making the periodic corrugations on the waveguide sidewall with a grating pitch Λ, the grating is produced. Fig.4(b) shows a zoom-in view of the gratings, in which it is clear to be seen that a spatial sampling with a spatial sampling period P is performed on the uniform Bragg grating. In the on-modulation grating region, the gratings maintain; and in the off-modulation grating region, there is no grating but the waveguide. To have an equivalent phase shift, an increase in the sampling period $P + \Delta L$ locates in the middle, where ΔL denotes the increase in the sampling period. To have an equival-

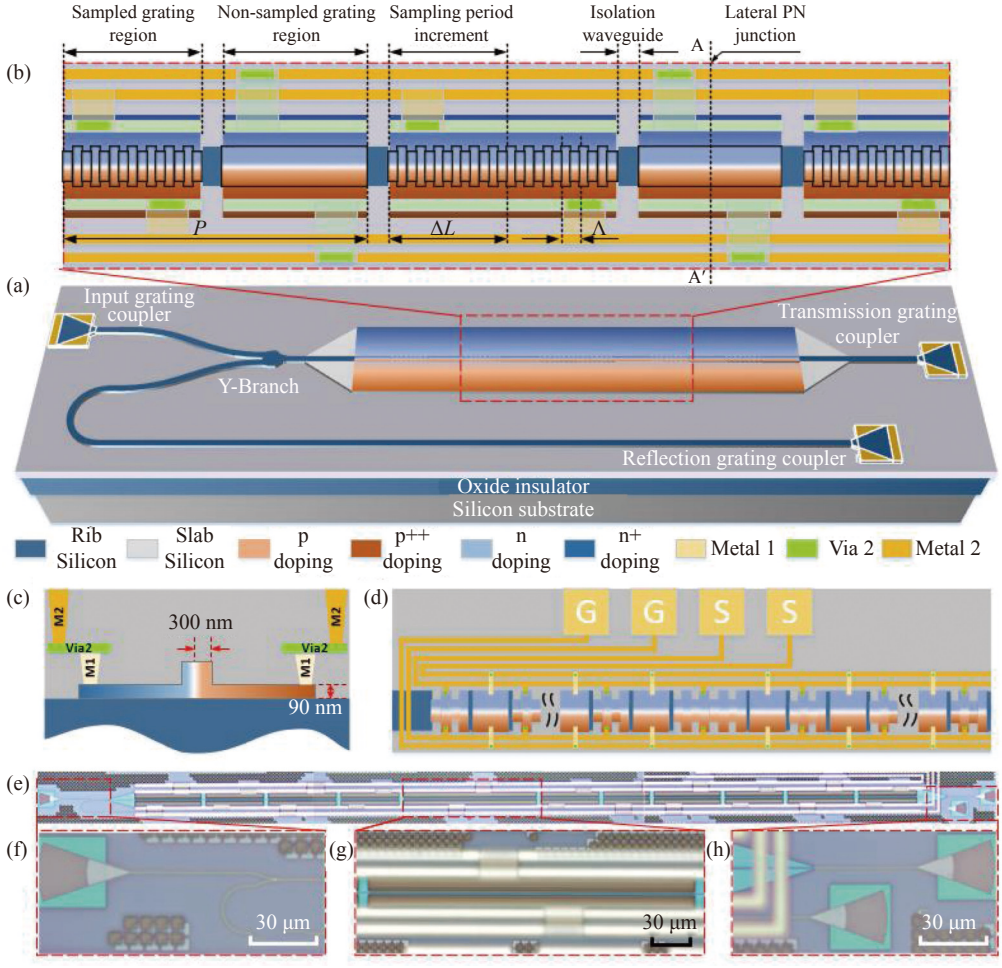

Fig. 4. (a) Schematic of a silicon-based reconfigurable EPS grating chip; (b) Grating design; (c) Lateral PN junction; (d) Grating metal connection; (e) Image of the fabricated grating; (f) Image of the input region; (g) Image of the increased sampling period ΔL; (h) Image of the output region.

ent phase-shift effect, the sampling period increase ΔL is equal to half of P. By introducing the spatial sampling profile, a new degree of freedom is created in the different grating implementation, which gives more room in the grating spectral tuning and highly reduces the fabrication tolerance.

To enable the proposed EPS grating electrically reconfigurable, the grating incorporates multiple lateral PN junctions. In Fig.4(b), there exists a sampled grating region and non-sampled grating region in a spatial sampling period, both of which are doped with an independent lateral PN junction. To avoid the electrical crosstalk between neighboring PN junctions, an electrical insulator is added with the use of a length of undoped waveguide. Fig.4(c) gives the lateral structure of the doped PN junction, in which the center of the PN junction is shifted from the waveguide center for high tuning efficiency. Fig.4(d) shows the top-view of the designed EPS waveguide grating, in which the PN junctions located in the sampled regions are bridged to have a common electrical contact, and the PN junctions located in the non-sampled grating regions are bridged to have a common electrical contact. Thus, with the use of the bias voltages control, the grating pitch Λ, the spatial sampling period P and the sampling period increment ΔL of the EPS waveguide grating can be tuned, which enables the full grating reconfigurability.

A programmable EPS waveguide grating is fabricated, and Fig.4(e) shows an image of the fabricated grating, of which the grating pitch is chosen to be 310 nm for C-band operation, and the spatial sampling period is 255.75 μm. Fig.4(f) gives a zoom-in view of the silicon grating coupler for input optical coupling. Fig.4(g) presents an image of the sampling period increase ΔL, which is equal to half of the spatial sampling period. Fig.4(h) shows the transmission and reflection output regions.

Fig.5(a) gives the static reflection spectra of the fabricated grating. Thanks to the spatial sampling, the EPS grating features a multi-channel spectral. And moreover, the increased sampling period has an equivalent phase shift effect on the odd-order channel spectra. It is clear to be seen that a passband happens in the transmission stopband and a notch exists in the reflection passband. This is exactly the typical spectral features of a phase-shifted Bragg grating. Fig.5(b) shows the zoom-in view of the grating negative-order channels spectra, in which the odd-order channels present EPS-resulted spectral features, while the even-order channels feature a shallow notch, which is caused by the leaking loss when the even-order optical modes are evanescently coupled into the cladding modes. Fig.5(c) shows the zoom-in view of the grating positive order channels spectra, in which the EPS-induced spectral features are apparently seen,

By controlling bias states of the PN junctions, different spectral responses of the fabricated waveguide grating can be realized. Fig.5(d) gives the spectral tun-

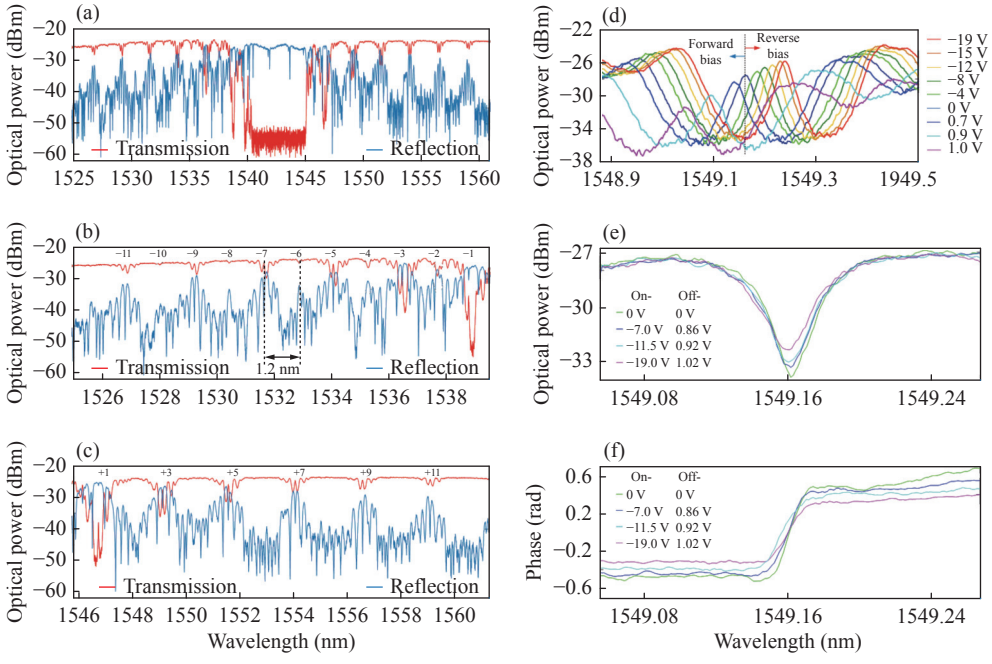

Fig. 5. (a) Static spectra of the fabricated grating; (b) Staci spectra of the grating negative-order channels; (c) Zoom-in static spectra of the grating positive-order channels; (d) Spectral tuning of the +3rd channel when all PN junctions are synchronously tuned; (e) Extinction ratio tuning and (f) Phase jump tuning of the +3rd channel reflection notch with the notch center maintains.

ing of the grating +3rd channel when the two bias voltages are synchronously tuned. When reverse biased, a red-shift happens to the spectrum; when forward biased, a blue-shift happens. In addition, the spectra wavelength shift caused by each junction could be canceled out with each other by independently tuning the two PN junctions. Thus, the grating wavelength remains the same, while the phase response and notch depth are tuned, as shown in Fig.5(e) and 5(f), respectively.

The proposed EPS waveguide grating features a programmable multi-channel spectral response, which paves the way for simultaneous manipulation of multiple wavelengths, thus enabling reconfigurable multichannel signal parallel processing. Especially, in a extensively-deployed WDM system, an EPS waveguide grating with a channel spacing compatible to the wavelength grid can be used to realize a programmable multichannel signal parallel processing functions including optical filtering, temporal differentiation and Hilbert transformation.

IV. Programmable Micro-Disk Resonator Array Photonic Signal Processor

Compared to the waveguide grating with a large size, an optical ring or disk cavity offers unique advantages including small footprint, strong wavelength selectivity and large functional flexibility, which are highly preferred by high-density and large-scale integrated microwave photonic processor circuits.

Fig.6(a) shows an image of an 8×8 photonic integrated field-programmable disk array (FPDA) signal processor [31]. The proposed signal processor has a two-dimensional mesh network with 8 optical input ports and 8 optical output ports. In the mesh cell, two high-Q micro-disk resonator (MDRs) with the identical design are employed to process, route and store optical signal. On top of each MDR, a metallic micro-heater is placed to tune the MDR, as seen in Fig.6(b), and Fig.6(e) gives the grating coupler image for I/O optical ports. By programming the voltages applied to the micro-heaters on top of each MDR, the different optical circuit topologies could be made to perform multiple tasks, and with a scalable configuration, the processor could be upgraded to have a strong parallel processing capacity, of which each independent task is specifically assigned to a dedicated region of the processor chip.

First, thanks to the wavelength selectivity of the MDR, it is straightforward to reconfigure the FPDA to be a flat-top optical filter by cascading two MDRs of which the resonance wavelengths are slightly apart. Fig.7(a) gives the measured spectral response of the optical filter, and Fig.7 (b) presents the measured

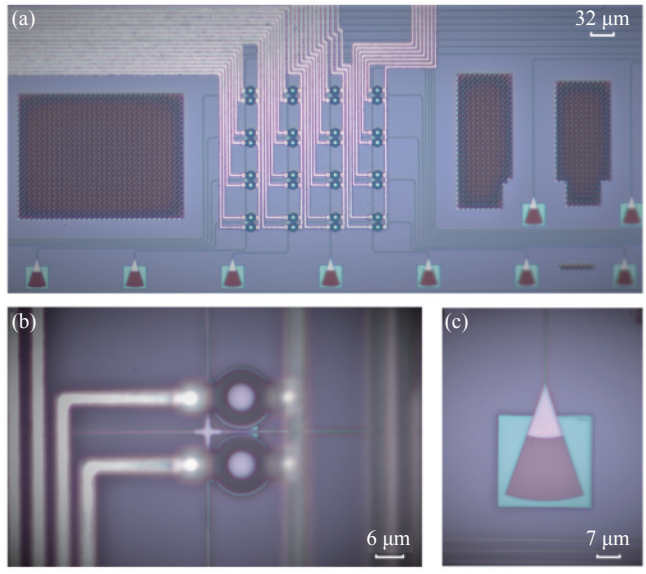

Fig. 6. (a) Image of an 8×8 photonic programmable signal processor; (b) Image of a single mesh cell; (c) Zoom-in view of the grating coupler for I/O optical coupling.

wavelength tunability of the filter by simultaneously controlling the two MDRs. With more MDRs incorporated, a higher out-of-band rejection ratio could be possible.

Thanks to its strong light-confining capacity, an MDR can store the optical signal to realize a delay line, and by cascading more MDRs, a wideband optical delay line is produced. Fig.7(c) presents the measured group delay of the fabricated FPDA as an optical delay line consisting of 8 cascaded MDRs. Fig.7 (d) shows the wavelength red-shifting of the delay line by changing the voltages applied to the micro-heaters on top of the MDRs based on thermal-optic effect.

In addition, due to the multiple MDRs, the fabricated FPDA can be used as an all-optical multichannel temporal differentiator, capable of performing temporal differentiation of multichannel signals in a WDM system. Fig.7 (e) gives an experimentally differentiated pulse when the center wavelength of the input optical Gaussian pulse is aligned to the notch wavelength of the third MDR (blue-solid line) and a theoretically differentiated Gaussian pulse (red-dashed line) for comparison. Fig.7 (f) gives an experimentally differentiated pulse when the center wavelength of the input optical Gaussian pulse is aligned to the notch wavelength of the eighth MDR (blue-solid line) and a theoretically differentiated Gaussian pulse (red-dashed line). The experimental results show that the experimental results are close to the theoretically simulations, which confirms the effectiveness of the device to realize fractional-order temporal differentiation.

To summarize, by controlling the MDRs, diverse

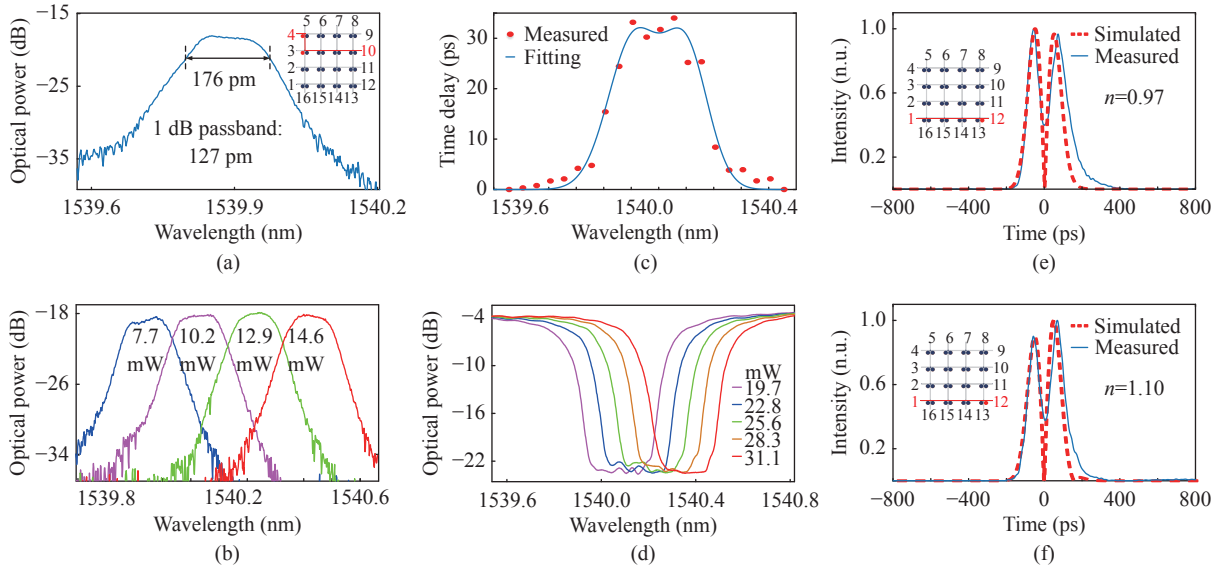

Fig. 7. (a) Measured spectral response of the flat-top optical filter; (b) Wavelength tunability of the flat-top optical filter; (c) Measured group delay of the delay line; (d) Wavelength tunability of the delay line; (e) Experimentally differentiated Gaussian pulse of the temporal optical differentiator; (f) Experimentally differentiated Gaussian pulse of another temporal optical differentiator.

circuit topologies of the FPDA could be realized, which could be used to perform different signal processing functions. In the experimental demonstration, several function including optical filtering, fractional-order temporal differentiation, true time delay, optical beamforming, and optical spectral shaping are achieved. Thanks to the small footprint and strong light-confining capacity of the MDRs, the signal processor holds the key advantages in terms of high scalability, full reconfigurability, strong parallel processing capability, and low power consumption.

V. Discussion and Conclusion

Silicon photonics is an excellent material platform to implement the on-chip integration of microwave photonic systems since it is compatible with mature CMOS technology. However, one key factor limiting the silicon for monolithic integration is the lack of optical sources and amplifiers, since silicon is a non-direct bandgap material. A potential solution is the heterogeneous integration which can integrate III-V optical sources and amplifiers on a silicon chip. The combination of the InP-based and silicon photonic PICs would significantly boost the performance of microwave photonic signal processor and opens up new avenues toward real applications.

An overview regarding our recent work on on-chip reconfigurable microwave photonic processor was discussed with an emphasis on silicon photonic implementations. With the high-speed silicon modulators with a low half-wave voltage [32], [33] and on-chip Germanium photodetectors with a high responsivity [34], [35] fully developed, as well as heterogeneous integration of III-V materials on silicon photonic chips [36], a promising prospect to realize a single-chip reconfigurable microwave photonic processor is coming.

References

[1] J. Capmany and D. Novak, " Microwave photonics combines two worlds," *Nature Photon.*, vol.1, no.6, pp.319–330, 2007.

[2] A. J. Seeds, "Microwave photonics," *IEEE Trans. Microw. Theory Tech.*, vol.50, no.3, pp.877–887, 2002.

[3] A. J. Seeds and K. J. Williams, "Microwave photonics," *J. Lightwave Technol.*, vol.24, no.12, pp.4628–4641, 2006.

[4] J. P. Yao, " Microwave Photonics," *J. Lightw. Technol.*, vol.27, no.3, pp.314–335, 2009.

[5] R. A. Minasian, " Photonic signal processing of microwave signals," *IEEE Trans. Microw. Theory Tech.* , vol.54, no.2, pp.832–846, 2006.

[6] R. A. Minasian, E. H. W. Chan, and X. Yi, "Microwave photonic signal processing," *Opt. Express* , vol.21, no.19, pp.22918–22936, 2013.

[7] J. Capmany, J. Mora, I. Gasulla, J. Sancho, "Microwave photonic signal processing," *J. Lightw. Technol.* , vol.31, no.4, pp.571–586, 2013.

[8] R. A. Minasian, "Ultra-wideband and adaptive photonic signal processing of microwave signals," *IEEE J. Quantum Electron.*, vol.52, no.1, pp.1–13, 2016.

[9] J. Capmany, B. Ortega, and D. Pastor, " A tutorial on microwave photonic filters," *J. Lightw. Technol.*, vol.24, no.1, pp.201–229, 2006.

[10] Y. Liu, Y. Yu, S. Yuan, X. Xu, and X. Zhang, "Tunable megahertz bandwidth microwave photonic notch filter based on a silica microsphere cavity," *Opt. Lett.* , vol.41, no.21, pp.5078–5081, 2016.

[11] J. Azaña, " Ultrafast analog all-optical signal processors based on fiber-grating devices," *IEEE Photon. J.* , vol.2, no.3, pp.359–386, 2010.

[12] M. Li, D. Janner, J. P. Yao, and V. Pruneri, "Arbitrary-order all-fiber temporal differentiator based on a fiber Bragg grating: Design and experimental demonstration," *Opt. Express*, vol.17, no.22, pp.19798–19807, 2009.
[13] H. Shahoei, P. Dumais, and J. P. Yao, "Continuously tunable photonic fractional Hilbert transformer using a high-contrast Germanium-doped silica-on-silicon microring resonator," *Opt. Lett.*, vol.39, no.9, pp.2778–2781, 2014.
[14] A. Altaqui, E. H. R. Chan, and R. A. Minasian, "Microwave photonic mixer with high spurious-free dynamic range," *Appl. Opt.*, vol.53, no.17, pp.3687–3695, 2014.
[15] Z. Z. Tang, Y. F. Li, J. P. Yao, and S. L. Pan, "Photonics-based microwave frequency mixing: methodology and applications," *Lasers Photon. Rev.* , vol.14, no.1, article no.1800350, 2020.
[16] W. Zhang and J. P. Yao, " Ultra-wideband RF photonic phase shifter using two cascaded polarization modulators," *IEEE Photon. Technol. Lett.*, vol.26, no.9, pp.911–914, 2014.
[17] S. Pan and Y. Zhang, " Tunable and wideband microwave photonic phase shifter based on a single-sideband polarization modulator and a polarizer," *Opt. Lett.* , vol.37, no.21, pp.4483–4485, 2012.
[18] H. Jiang, L. Yan, J. Ye, *et al.*, "Tunable microwave photonic pulse shaping based on modified incoherent frequency-to-time mapping," in *Proceedings of 2012 IEEE International Topical Meeting on Microwave Photonics*, Noordwijk, Netherland, pp.240–243, 2012.
[19] E. Hamidi, D. E. Leaird, and A. M. Weiner, "Tunable programmable microwave photonic filters based on an optical frequency comb," *IEEE Trans. Microw. Theory Tech.*, vol.58, no.11, pp.3269–3278, 2010.
[20] H. Chi, F. Zeng, and J. Yao, " Photonic generation of microwave signals based on pulse shaping," *IEEE Photon. Technol. Lett.*, vol.19, no.9, pp.668–670, 2007.
[21] J. Zhang and J. P. Yao, " Photonic true-time delay beamforming using a switch-controlled wavelength-dependent recirculating loop," *J. Lightw. Technol.* , vol.34, no.16, pp.3923–3929, 2016.
[22] D. Marpaung, C. Roeloffzen, R. Heideman, *et al.*, "Integrated microwave photonics," *Lasers Photon. Rev.* , vol.7, no.4, pp.506–538, 2013.
[23] W. Zhang and J. P. Yao, " Silicon-based integrated microwave photonics," *IEEE J. Quantum Electron.*, vol.52, no.1, article no.0600412, 2016.
[24] D. Marpaung, J. P. Yao, and J. Capmany, "Integrated microwave photonics," *Nature Photon.*, vol.13, no.1, pp.80–90, 2019.
[25] J. P. Yao and W. Zhang, "Silicon photonic integrated waveguide Bragg gratings and applications in programmable photonic signal processing," *J. Lightw. Technol.* , vol.38, no.2, pp.202–214, 2020.
[26] L. Zhuang, C. Roeloffzen, M. Hoekman, *et al.*, "Programmable photonic signal processor chip for radiofrequency applications," *Optica*, vol.2, no.10, pp.854–859, 2015.
[27] D. Prez, I. Gasulla, L. Crudgington, *et al.*, "Multipurpose silicon photonics signal processor core," *Nature Commun.*, vol.8, article no.636, 2017.
[28] W. Liu, M. Li, R. S. Guzzon, *et al.*, "A fully reconfigurable photonic integrated signal processor," *Nature Photon.*, vol.10, no.3, pp.190–195, 2016.
[29] W. Zhang and J. P. Yao, "A fully reconfigurable waveguide Bragg grating for programmable photonic signal processing," *Nature Comm.*, vol.9, article no.1396, 2018.
[30] W. Zhang and J. P. Yao, " Electrically programmable on-chip equivalent-phase-shifted waveguide Bragg grating on silicon," *J. Lightw. Technol.*, vol.37, no.2, pp.314–322, 2019.
[31] W. Zhang and J. P. Yao, " Photonic integrated field-programmable disk array signal processor," *Nature Comm.*, vol.11, article no.406, 2020.
[32] D. Thomson, F. Gardes, Y. Hu, *et al.*, " High contrast 40 Gbit/s optical modulation in silicon," *Opt. Express*, vol.19, no.12, pp.11507–11516, 2011.
[33] F. Gardes, A. Brimont, P. Sanchis, *et al.*, "High-speed modulation of a compact silicon ring resonator based on a reverse-biased pn diode," *Opt. Express* , vol.17, no.24, pp.21986–21991, 2009.
[34] M. W. Geis, S. J. Spector, M. E. Grein, *et al.*, "Silicon waveguide infrared photodiodes with >35 GHz bandwidth and phototransistors with 50 AW-1 response," *Opt. Express*, vol.17, no.7, pp.5193–5204, 2009.
[35] D. Ahn, C.-Y. Hong, J. Liu, *et al.*, " High performance, waveguide integrated Ge photodetectors," *Opt. Express*, vol.15, no.7, pp.3916–3921, 2007.
[36] A. W. Fang, H. Park, O. Cohen, *et al.*, "Electrically pumped hybrid AlGaInAs-silicon evanescent laser," *Opt. Express*, vol.14, no.20, pp.9203–9210, 2006.

ZHANG Weifeng was born in Henan Province, China. He received the B.E. degree in electronic science and technology from Xi'an Jiaotong University, Xi'an, China, in 2008, the M.S. degree in electrical engineering from the Politecnico di Torino, Turin, Italy, in 2011, and the Ph.D. degree in electrical engineering from the University of Ottawa, Ottawa, ON, Canada, in 2017. From June 2017 to May 2019, he was a Postdoctoral Fellow with the University of Ottawa. In June 2019, he joined the School of Information and Electronics, Beijing Institute of Technology, Beijing, China, as a Full Professor. His current research focuses on opto-electric detection and identification, including integrated microwave photonic chips, photonic computing chips, and 3D lidar imaging chips.
(Email: weifeng.zhang@bit.edu.cn)

WANG Bin was born in Hunan Province, China. He received the B.E. degree in communication engineering from Huazhong University of Science and Technology, China, in 2014 and the Ph.D. degree in electronic science and technology from Shanghai Jiao Tong University, Shanghai, China, 2020. From September 2018 to September 2019, he was a joint training Ph.D. student with the University of Ottawa, Ottawa, ON, Canada. In May 2020, he joined the School of Information and Electronics, Beijing Institute of Technology, Beijing, China, as an Assistant Professor. His current research interests include integrated microwave photonic chips and microwave photonic radar systems.